HHS Public Access

Author manuscript

Am J Med Genet A. Author manuscript; available in PMC 2018 December 01.

Published in final edited form as:

Am J Med Genet A. 2017 December ; 173(12): 3221–3225. doi:10.1002/ajmg.a.38415.

A Novel Missense Variant in the GLI3 Zinc Finger Domain in a Family with Digital Anomalies

J. Aaron Crapster[1], **Louanne Hudgins**[2], **James K. Chen**[1,3], and **Natalia Gomez-Ospina**[2,*]

[1]Department of Chemical and Systems Biology; Stanford University School of Medicine, Stanford, CA 94305, USA

[2]Division of Medical Genetics; Stanford University School of Medicine, Stanford, CA 94305, USA

[3]Department of Developmental Biology; Stanford University School of Medicine, Stanford, CA 94305, USA

Abstract

Mutations in *GLI3*, which encodes a transcription factor of the Hedgehog signaling pathway, cause several developmental anomalies linked to inappropriate tissue patterning. Here, we report a novel missense variant in the fifth zinc finger domain of *GLI3* (c.1826G>A; p.(Cys609Tyr)) initially identified in a proband with preaxial polydactyly type IV, developmental delay, sensorineural hearing loss, skeletal, and genitourinary anomalies. Additional family members exhibited various digital anomalies such as preaxial polydactyly, syndactyly, and postaxial polydactyly either in isolation or combined. Functional studies of Cys609Tyr GLI3 in cultured cells showed abnormal GLI3 processing leading to decreased GLI3 repressor production, increased basal transcriptional activity, and submaximal GLI reporter activity with Hedgehog pathway activation, thus demonstrating an intriguing molecular mechanism for this GLI3-related phenotype. Given the complexity of GLI3 post-translational processing and opposing biological functions as a transcriptional activator and repressor, our findings highlight the importance of performing functional studies of presumed *GLI3* variants. This family also demonstrates how *GLI3* variants are variably expressed.

Keywords

GLI3; Greig cephalopolysyndactyly; Pallister-Hall; polydactyly; Zinc finger domain

INTRODUCTION

GLI3 is one of three GLI transcription factors of the canonical Hedgehog (HH) signaling pathway, and is an essential regulator of development and tissue patterning [Hui and Angers, 2011]. Numerous pathogenic variants of the *GLI3* gene have been linked to complex clinical phenotypes. GLI3-related phenotypes include Greig cephalopolysyndactyly syndrome (GCPS, MIM175700), Pallister-Hall syndrome (PHS, MIM146510), non-syndromic postaxial polydactyly type A1 and B (PAP-A/B, MIM174200), and preaxial polydactyly

*Corresponding author: gomezosp@stanford.edu.

type IV (PPD-IV, MIM174700) [Biesecker, 2006]. Classic GCPS is characterized by the triad of widely spaced eyes, macrocephaly, and PPD-IV or mixed pre- and postaxial polysyndactyly in at least one limb [Balk and Biesecker, 2008; Johnston et al., 2010]. Pallister-Hall syndrome is described as an association of mesoaxial or PAP-A/B with hypothalamic hamartoma, though patients can also present with some combination of bifid epiglottis, non-digit skeletal defects, anorectal or genitourinary malformations, and sensorineural hearing loss (SNHL) [Hall et al., 1980; Johnston et al., 2010; Narumi et al., 2010]. Mild forms of GCPS and PHS can also be incorrectly diagnosed as isolated polydactyly and syndactyly.

GLI3 contains several functional domains, including an N-terminal transcriptional repressor and two C-terminal transcriptional activation domains, endowing GLI3 with dual and opposing functional capabilities (Figure 1A, [Hui and Angers, 2011]. In the central region of GLI3, there are five C2H2-type zinc fingers that mediate DNA binding, and a domain that mediates GLI3 proteolytic processing. In the absence of HH signaling, GLI3 is post-translationally processed into an N-terminal transcriptional repressor (GLI3R). Hedgehog pathway activation blocks GLI3R formation and stimulates the conversion of full-length GLI3 into a transcriptional activator (GLI3A). GLI3A then acts along with other GLI transcription factors (GLI1 and GLI2) to promote HH target gene expression. Maintaining the appropriate balance between full-length GLI3 activator and truncated GLI3 repressor is critical for tissue patterning during development.

Consistent with their distinct phenotypes, GCPS and PHS patients can be categorized by discrete sets of genotypes that differentially affect GLI3 function (Figure 1A) [Johnston et al., 2010; Jamsheer et al., 2012; Demurger et al., 2015]. The GCPS phenotype is proposed to result from GLI3 haploinsufficiency, due to exonic or gene deletions, early truncation, loss of DNA binding (including point mutations in the Zinc finger domains) as well as loss of transactivation. In contrast, changes that result in a constitutive GLI3R activity are thought to result in PHS [Kalff-Suske et al., 1999; Johnston et al., 2010].

Here, we report a novel *GLI3* missense variant in a family that caused a spectrum of digital anomalies. All affected individuals that were tested harbored a c.1826G>A (p.(Cys609Tyr)) variant in *GLI3*. Functional studies of the murine p.Cys609Tyr GLI3 showed that the mutant protein is not efficiently processed to GLI3R, resulting in a full-length protein with basal transcriptional activity and submaximal pathway activation.

MATERIALS AND METHODS

Patients

Subjects were enrolled in a research study approved by the institutional review boards of Stanford University School of Medicine.

GLI3 Sequencing

Clinical sequencing of *GLI3* for the proband was performed through Prevention Genetics laboratories (Wisconsin, USA). For other individuals, genomic DNA was extracted from

saliva, the region of interest was amplified by PCR, purified and sequenced using standard techniques.

Plasmid Construction

The p3xFLAG-GLI3 and p3xFLAG-GLI3R expression constructs were previously described [Rack et al., 2014]. The p3xFLAG-GLI3C609Y construct was generated using standard site-directed mutagenesis.

Luciferase Reporter Assays

Gli3$^{-/-}$ mouse embryonic fibroblast (MEF) cells were provided by W. Bushman (University of Wisconsin-Madison) and were cultured using standard media. The cells were transfected with control or p3xFLAG-GLI3, p8xGliBS-FL (GLI-dependent firefly luciferase), and phRL-SV40 (constitutive *Renilla* luciferase). Luciferase activities were measured using a Dual-Luciferase Reporter system (Promega) on a luminometer (Veritas).

Immunoblotting

Transfected Gli3$^{-/-}$ MEFs were lysed 48 or 72 h after transfection and western blotting was performed using a standard protocol. GLI3 was detected using anti-GLI3 primary antibody (goat polyclonal, R&D systems, AF3690), and HRP-conjugated bovine anti-goat secondary antibody (Jackson ImmunoResearch, 805-035-180). Band intensities were quantified using ImageJ software.

For full details on sequencing, plasmids, luciferase reporter assays and immunoblotting, see supplementary online material.

RESULTS

Clinical Report

The proband was a five-year-old first-born daughter of unrelated Mexican-American parents at the time of our examination. She was delivered at 28 weeks by cesarean due to severe ascites. Her growth parameters adjusted for gestational age were: weight =1.249 g (79th centile) and length =35.5 cm (45th centile). The ascites was due to a cloacal anomaly consisting of absent urethral and vaginal openings and an anteriorly placed anus. She also had a tethered cord. She spent the first three months in the intensive care unit. Her urogenital anomalies were repaired, and at five years of age she was potty-trained for stool but had persistent encopresis and a neurogenic bladder. She had asymmetric kidneys, with the right kidney shorter than the left. Skeletal anomalies included 13 ribs on both sides and a protruding lower rib cage on the left. She had moderate-to-severe bilateral SNHL, as well as mild motor and language delays. On exam, she was found to have widely spaced eyes (Interpupillary distance (IPD)= 6.5 cm; >97th centile [Gripp, 2013]), a prominent forehead and wide nasal bridge, and toe anomalies consisting of left PPD-IV, right broad hallux, 2–3 toe cutaneous syndactyly and bilateral short and overlapping fourth toes (Figure 1B, III.9). Her OFC was within normal limits for age (51cm; 58th centile).

The proband's father (II.4, Figure 1B) was born with PAP-B of the left hand and bilateral preaxial polydactyly of the feet, which were repaired. On exam, he was found to have, in addition to post-surgical changes, left 2–3 cutanous syndactyly of the toes and medial deviation of the third toes. His eyes appeared normally spaced and he was normocephalic (OFC = 58 cm; 75th centile). Family history included multiple family members with digit anomalies comprised of unilateral hand PAP-A (III.2), mixed PAP-A of the hands, PPD-IV and syndactyly of the feet respectively (I.1, II.1, II.2, III.11), or isolated preaxial polydactyly of the feet (II.7, III.3, III4, III.6, and III.9). Facial features from photographs of II.1–8 and III.4 were unremarkable, specifically eye spacing and head size were subjectively normal.

Due to the family history of digit anomalies, a diagnosis of PPD-IV was considered. Sanger sequencing of the *GLI3* gene idnetified a novel c.1826G>A variant (p.(Cys609Tyr)) in the proband (NM_000168.5, Supplemental Figure 1). The variant was absent in ExAC and was predicted to be deleterious based on three amino acid substitution programs. Parental testing showed the variant was paternally inherited (II.4). Familial testing for the variant on individuals II.2, II.6, II.7, III.4 found that the three relatives with digit anomalies were also heterozygous for c.1826G>A, while unaffected family members were wild type (Figure 1B).

Functional studies of the GLI3 p.Cys609Tyr variant

The C2H2 zinc finger DNA-binding regions of GLI3 are highly conserved across the mammalian class (Figure 1C), suggesting that the Cys609Tyr amino acid change could be deleterious [Takafumi et al., 2003]. To understand the effect of this missense change in protein function, we used site-directed mutagenesis to create the murine variant, and transiently overexpressed it in cultured mouse embryonic fibroblasts lacking endogenous *Gli3* (*Gli3*$^{-/-}$ MEFs). The cells were also co-transfected with a GLI-dependent firefly luciferase reporter, and then cultured in the absence or presence of SHH-N ligand. Due to loss of GLI3R function, *Gli3*$^{-/-}$ MEFs exhibit constitutive HH pathway activity, which can be enhanced further with SHH-N stimulation. As expected, overexpression of either wild type GLI3 or GLI3R inhibited both basal and SHH-N-stimulated GLI reporter activity in these cells, with GLI3R exhibiting a greater suppressive effect (Figure 1D). Surprisingly, the GLI3 p.Cys609Tyr variant moderately elevated GLI reporter levels in non-stimulated *Gli3*$^{-/-}$ MEFs relative to the EGFP control, indicating that the mutant acts primarily as a transcriptional activator rather than a repressor. Consistent with this result, western blot analyses of the transfected *Gli3*$^{-/-}$ MEFs demonstrated that overexpressed wild type GLI3 is processed efficiently into GLI3R, but the Cys609Tyr mutant is not (Figure 1E). However, we also observed that expression of GLI3 p.Cys609Tyr prevented maximal SHH-N-induced GLI reporter activity in comparison to EGFP (Figure 1D). Taken together, these results suggest that the Cys609Tyr mutant is a weak transcriptional activator that might competitively suppress HH target gene expression mediated by the other GLI proteins.

DISCUSSION

By genotyping a large family with digit anomalies, we identified a novel c.1826G>A variant in *GLI3*. The pathogenicity of this variant is supported by: 1) its absence from population databases, 2) its co-segregation with affected kindred, 3) multiple computational programs

predicted as deleterious, 4) its location in a critical and well-established functional domain of the protein, and 5) its abnormal transcriptional activity and proteolytic processing in functional studies. Accordingly, this variant can be conservatively classified as likely pathogenic [Richards et al., 2015]. The phenotype was found to have variable expressivity. Expect for the proband, family members had only apparent digit anomalies. However, mild forms of GCPS could have been missed due to the lack of comprehensive phenotyping of all individuals.

Cysteine 609 is one of the residues that directly coordinates a Zn^{2+} ion in the fifth zinc finger domain of GLI3. Accordingly, the p.Cys609Tyr variant would be expected to have diminished DNA binding, as postulated for a similar GLI3 variant, p.His601Arg [Volodarsky et al., 2014]. Since GLI3 has both transcriptional repressor and activator functions, disrupting a zinc finger domain could interfere with either or both activities. Expression of GLI3 p.Cys609Tyr in cultured MEFs lacking endogenous *Gli3* showed that the mutant protein increased basal levels of GLI-dependent transcription, an observation potentially explained by the inability of GLI3 mutant to be processed into its repressor form. To our knowledge, a role for the zinc finger domains in the regulation of GLI3 post-translational processing has not been previously reported. The fifth zinc finger domain is proximal to the processing domain, and we speculate that the Cys609Tyr mutation may lead to conformational changes that impede processing domain recognition and GLI3 proteolysis.

We propose that individuals heterozygous for *GLI3* c.1826G>A could be functionally haploinsufficient with respect to GLI3R, explaining why the proband and other affected family members in this study have the limb anomalies more typically described in GCPS. Our data further suggest that the Cys609Tyr mutation not only abrogates GLI3R production, but generates a weak transcriptional activator that can possibly competitively inhibit GLI2 and GLI1 function in cells.

The proband had additional findings of SNHL, non-digit skeletal anomalies, renal, and genital malformations. One explanation is that the additional findings are unrelated to the *GLI3* variant. An alternative hypothesis is that the proband may have additional genetic or environmental factors that suppressed HH signaling function in the affected tissues, which in combination with the *GLI3* c.1826G>A allele contributed to a more severe phenotype. This is not unreasonable given these anomalies have been reported in PHS. This study highlights the complicated biology of HH pathway transcription factors and demonstrates the importance of conducting functional experiments when describing *GLI3* mutations. Amino acid changes in well-defined domains may in fact influence GLI3 protein function in unexpected ways.

Supplementary Material

Refer to Web version on PubMed Central for supplementary material.

Acknowledgments

We gratefully acknowledge the family members who participated in this study. This work was supported by the National Institutes of Health (R01 GM113100 to J. K. C.) and an American Cancer Society Postdoctoral Fellowship (J.A.C.)

References

Balk K, Biesecker LG. The clinical atlas of greig cephalopolysyndactyly syndrome. American Journal of Medical Genetics Part A. 2008; 146A(5):548–557. [PubMed: 18241058]

Biesecker LG. What you can learn from one gene: Gli3. Journal of Medical Genetics. 2006; 43(6): 465–469. [PubMed: 16740916]

Demurger F, Ichkou A, Mougou-Zerelli S, Le Merrer M, Goudefroye G, Delezoide AL, Quelin C, Manouvrier S, Baujat G, Fradin M, et al. New insights into genotype-phenotype correlation for gli3 mutations. European Journal of Human Genetics. 2015; 23(1):92–102. [PubMed: 24736735]

Gripp, KW. Handbook of physical measurements. Oxford ; New York, NY: Oxford University Press; 2013.

Hall JG, Pallister PD, Clarren SK, Beckwith JB, Wiglesworth FW, Fraser FC, Cho S, Benke PJ, Reed SD, Optiz JM. Congenital hypothalamic hamartoblastoma, hypopituitarism, imperforate anus, and postaxial polydactyly—a new syndrome? Part i: Clinical, causal, and pathogenetic considerations. American Journal of Medical Genetics. 1980; 7(1):47–74. [PubMed: 7211952]

Hui CC, Angers S. Gli proteins in development and disease. Annual Review of Cell and Developmental Biology. 2011; 27:513–537.

Jamsheer A, Sowińska A, Trzeciak T, Jamsheer-Bratkowska M, Geppert A, Latos-Bieleńska A. Expanded mutational spectrum of the gli3 gene substantiates genotype–phenotype correlations. Journal of Applied Genetics. 2012; 53(4):415–422. [PubMed: 22903559]

Johnston JJ, Sapp JC, Turner JT, Amor D, Aftimos S, Aleck KA, Bocian M, Bodurtha JN, Cox GF, Curry CJ, et al. Molecular analysis expands the spectrum of phenotypes associated with gli3 mutations. Human Mutation. 2010; 31(10):1142–1154. [PubMed: 20672375]

Kalff-Suske M, Wild A, Topp J, Wessling M, Jacobsen E-M, Bornholdt D, Engel H, Heuer H, Aalfs CM, Ausems MGEM, et al. Point mutations throughout the gli3 gene cause greig cephalopolysyndactyly syndrome. Human Molecular Genetics. 1999; 8(9):1769–1777. [PubMed: 10441342]

Narumi Y, Kosho T, Tsuruta G, Shiohara M, Shimazaki E, Mori T, Shimizu A, Igawa Y, Nishizawa S, Takagi K, et al. Genital abnormalities in pallister–hall syndrome: Report of two patients and review of the literature. American Journal of Medical Genetics Part A. 2010; 152A(12):3143–3147. [PubMed: 21108399]

Rack PG, Ni J, Payumo AY, Nguyen V, Crapster JA, Hovestadt V, Kool M, Jones DTW, Mich JK, Firestone AJ, et al. Arhgap36-dependent activation of gli transcription factors. Proceedings of the National Academy of Sciences. 2014; 111(30):11061–11066.

Richards S, Aziz N, Bale S, Bick D, Das S, Gastier-Foster J, Grody WW, Hegde M, Lyon E, Spector E, et al. Standards and guidelines for the interpretation of sequence variants: A joint consensus recommendation of the american college of medical genetics and genomics and the association for molecular pathology. Genetics in Medicine. 2015; 17(5):405–424. [PubMed: 25741868]

Takafumi N, Makiko S, Kiyoshi A. Correlated mutation analysis of c2h2 zinc finger domains. Genome Informatics. 2003; 14:565–566.

Volodarsky M, Langer Y, Birk OS. A novel gli3 mutation affecting the zinc finger domain leads to preaxial-postaxial polydactyly-syndactyly complex. BMC Medical Genetics. 2014; 15(1):110. [PubMed: 25267529]

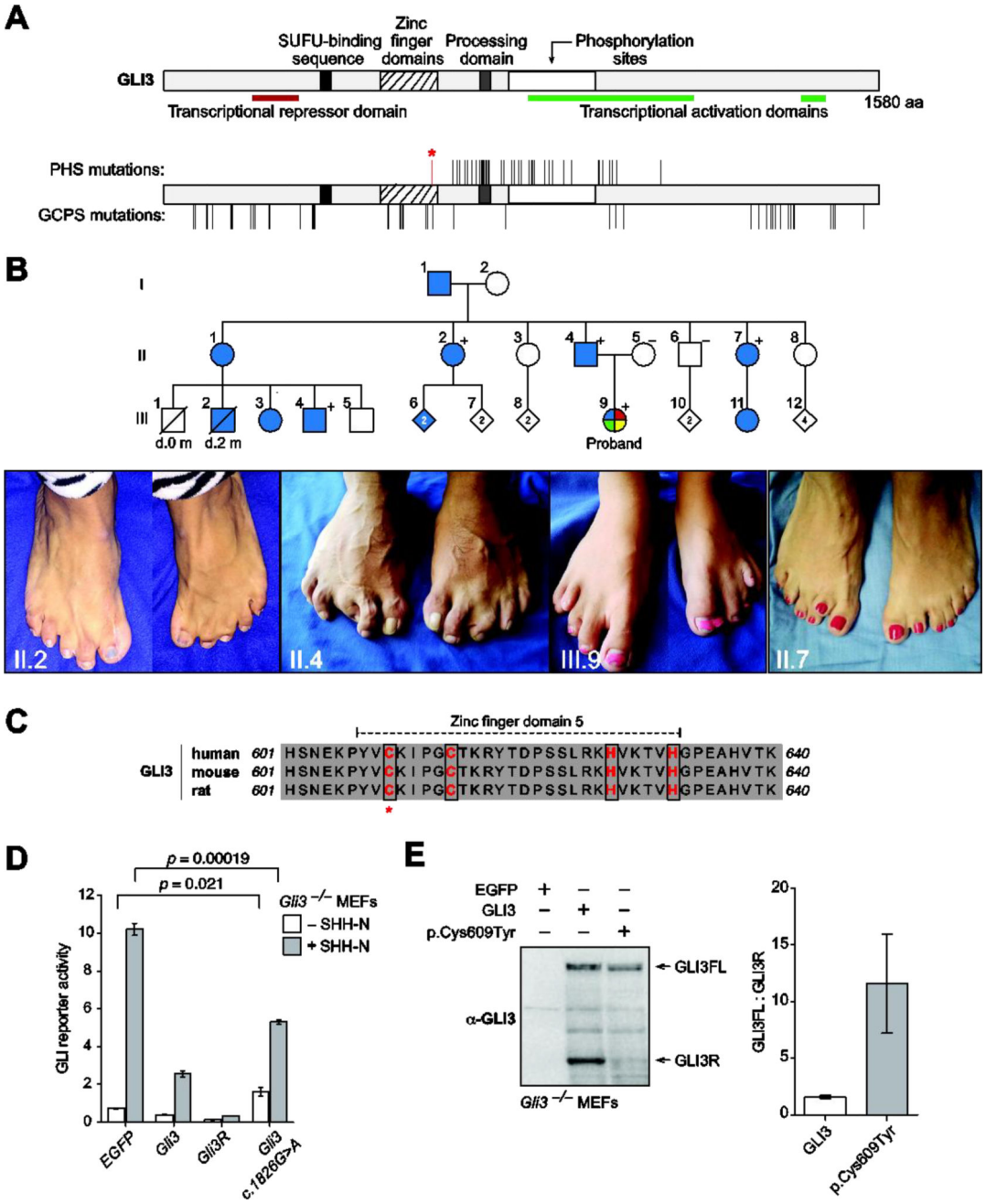

Figure 1. Identification and Functional Studies of GLI3 p.Cys609Tyr

(A) The top diagram, shows relevant functional domains of GLI3. The bottom diagram indicates exon mutations known to cause GCPS or PHS by vertical lines (Adapted from [Johnston et al., 2010; Jamsheer et al., 2012]). GLI3 p.Cys609Tyr is denoted with an asterisk. (B) Family tree of the kindred studied in this report (Color version: blue = digit anomalies, red = genitourinary anomalies, green = skeletal anomalies, yellow = sensorineural hearing loss. Monochrome version: black = digit anomalies, darkest gray = genitourinary anomalies, mid gray = skeletal anomalies, light gray = sensorineural hearing loss); toe anomalies of selected family members are depicted, and all phenotypes are

described in more detail in the text. (C) Sequence alignment of the fifth zinc finger domain of GLI3 shows homology across mammalian species. Cysteine 609 is indicated by an asterisk. (D) HH pathway activities in *Gli3*$^{-/-}$ MEFs co-transfected with a GLI-dependent firefly luciferase reporter, a constitutive *Renilla* luciferase reporter, and the designated cDNA constructs. Reporter activities (relative to transfection of an empty vector) in the absence and presence of SHH-N stimulation for 30 h are shown. Data are the average of quadruplicate samples ± SEM, and are representative of four experiments. (E) GLI3 processing in *Gli3*$^{-/-}$ MEFs transfected with either EGFP, GLI3, or GLI3 p.Cys609Tyr for 48 h. A representative blot is shown, and protein bands corresponding to the different GLI3 protein states are labeled. An equivalent amount of total protein was loaded into each lane, and quantification of the GLI3FL:GLI3R ratios is shown (data from three independent experiments ± SEM).